Analytica Chimica Acta xxx (2016) 1–8

Contents lists available at ScienceDirect

Analytica Chimica Acta

journal homepage: www.elsevier.com/locate/aca

Glycated hemoglobin biosensing integration formed on Au nanoparticle-dotted tubular TiO_2 nanoarray☆

Utkarsh Jain [a], Anamika Singh [b], Naresh Kumar Kuchhal [c], Nidhi Chauhan [a, *]

[a] Amity Institute of Nanotechnology, Amity University, Noida, 201303, Uttar Pradesh, India
[b] Department of Biotechnology, UIET, Kurukshetra University, Kurukshetra, 136 119, Haryana, India
[c] Clinical Biochemistry Department, Bio-Diagnostics, Rohini, Delhi, 110085, India

HIGHLIGHTS

- Fabrication of a highly sensitive and stable sensing interface consisting of gold nanoparticles (GNPs) and tubular TiO2.
- Biosensor exhibited low detection limit (0.5 μM).
- The half life of electrode was 4 months.
- Biosensor was suitable for detection of glycated hemoglobin in whole blood.

GRAPHICAL ABSTRACT

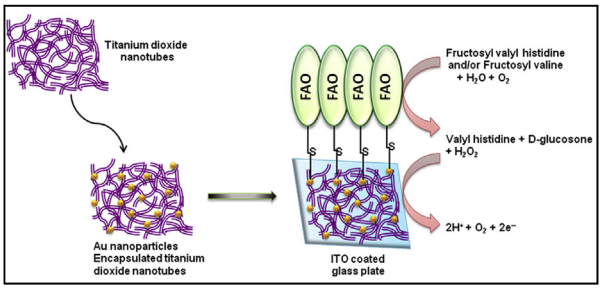

ARTICLE INFO

Article history:
Received 15 July 2016
Received in revised form
18 September 2016
Accepted 26 September 2016
Available online xxx

Keywords:
Gold nanoparticle
TiO_2 nanotubes
ITO electrode
Glycated hemoglobin

ABSTRACT

Excessive glucose present in the blood of diabetic patients binds with the hemoglobin of red blood cells resulting in the formation of glycated hemoglobin (HbA_{1c}). Measurement of HbA_{1c} levels may help in identifying the efficacy of the ongoing treatment and hence provide a better control over the disease. In the present study, we have synthesized a sensitive and stable scaffold, which consists of Au nanoparticles (GNPs)-dotted tubular TiO_2, for the construction of an electrochemical HbA_{1c} biosensor. 12-phosphotungstic acid has been used as a reducer after depositing well-dispersed GNPs on TiO_2 nanotubes (TiO_2 NTs) and an electron mediator by accelerating the electron transfer between the conductor and protein. The fabricated electrode was characterized using scanning electron microscopy (SEM), cyclic voltammetry (CV), Fourier transform infrared spectroscopy (FTIR) and electrochemical impedance spectroscopic analysis (EIS). Biosensor exhibited low detection limit (0.5 μM), fast response time (3 s) and wide linearity (from 0.5 to 2000 μM). The working electrode was used 100 times over 4 months, when stored at 4 °C. The HbA1c biosensor was then effectively used to measure the % of HbA_{1c} in the blood of apparently healthy persons and diabetic patients.

1. Introduction

The rod morphology nanostructures, TiO_2 nanotubes (NTs), are potent nanomaterials used in the development of highly sensitive devices for application in optics [1,2], electronics [3] and catalysis [4] due to their low dimensionality and unique properties. They are different from bulk structures, thin films and spherical particles [5].

☆ Selected paper from the 9th International Conference on Instrumental Methods of Analysis-Modern Trends and Applications, 20–24 September 2015 in the city of Kalamata on the Peloponnese Peninsula in Greece.

* Corresponding author.
E-mail address: nidhichauhan2007@rediffmail.com (N. Chauhan).

http://dx.doi.org/10.1016/j.aca.2016.09.026
0003-2670/

Factors responsible for better analytical performance of TiO_2 NTs sensors are high specific surface area, improved biocompatibility and improved conductivity through their cylindrical geometry [6–8]. The inner surface area of the TiO_2 NTs facilitates stable enzyme immobilization resulting in enhancement of proper performance of the nano-biosensors in comparison to the spherical and bulkier nanoparticles [9]. Nanocomposites made of TiO_2 NTs along with gold nanoparticles (GNPs) for construction of enzyme sensors have been previously reported [8,10]. GNPs not only provide a desirable microenvironment for the biomolecules [11] but also promote electron transfer by acting as a bridge between electrode support and redox proteins [12,13]. In the current work, we have employed GNPs–dotted tubular TiO_2 nanocluster for electrochemical detection of glycated hemoglobin (HbA_{1c}). HbA1c, a form of hemoglobin, is produced when glucose undergoes Amadori rearrangement reaction with the N-terminal valine of one or both the beta chains of hemoglobin [14]. Rate of HbA_{1c} formation is directly proportional to the concentration of glucose in blood stream. Hence, the amount of HbA_{1c} present in the erythrocytes is an indicator of the mean blood glucose concentration over the average life span of an erythrocyte (~120 days). Thus, it might be used as a tool to monitor a patient's metabolism over an extended period of 2 months [15]. HbA_{1c} levels are usually reported as the % fraction of the total hemoglobin. The normal range for HbA_{1c} is 5–15%. American Diabetes Association (ADA) has recommended that the HbA_{1c} level should be maintained below 6.5% and a patient must be kept on a specific control regime if the HbA_{1c} level exceeds than 6.5%. Each one percent increase in HbA_{1c} concentration is corresponding to a 2 mM increase in the concentration of mean blood glucose [16]. The measurements of HbA_{1c} have been performed by various techniques including immunoassay [17], boronate affinity chromatography [18], ionexchange chromatography [19], piezoelectric methods [20], colorimetry [21] and mass spectroscopy [22]. However, these techniques involve complex analytical procedures; require detection labels and pretreatment of proteins. In comparison to the above techniques, amperometric quantification methods have many advantages such as high sensitivity, good selectivity, relatively low cost and the possibility for miniaturization [23,24]. Hence, an electrochemical biosensor for the measurement of HbA_{1c} level is highly suitable for point-of care (POC) application.

In the present work, we have developed an amperometric biosensor for HbA_{1c} measurement in whole blood. Polyoxometalate anion of 12-phosphotungstic acid (PTA) was used as a linker to attach GNPs to TiO_2 NTs. Fructosyl-amino acid oxidase (FAO) was immobilized on the resulting scaffold to construct a working electrode. PTA reduced photochemically first acts as a localized reducing agent to deposit GNPs on TiO_2 NTs surface and later as an electron intermediate to improve the catalytic reaction of enzyme. It also increases the long term stability of the sensor. In order to increase electron transfer directly at the biosensor interface, it is required to support the contact between FAO and GNPs-PTA modified TiO_2 NTs. One way to accomplish this is by attaching a sulfhydryl group to FAO using a dithio cross-linker so that it can strongly attach to the GNPs. Therefore, a good interaction between GNPs and thiolated FAO is expected to improve the stability of FAO in this scaffold.

2. Experimental

2.1. Chemicals and reagents

Fructosyl-aminoacid oxidase (FAO, EC 1.5.3, 0.45 Umg^{-1} from recombinant *Escherichia coli*) was procured from Sigma-Aldrich, USA. 12-phosphotungstic acid (PTA), L-valine, pyridine, CHES (2-(Cyclohexylamino) ethanesulfonic acid), Triton X 100, SDS (Sodium dodecyl-sulfate), dess martin periodinane, dithio-threitol (DTT), MES (4-Morpholinoethane sulfonic acid), 4-aminoantipyrine, purified *Bacillus* sp. Proteases, *N*-succinimidyl 3-(2-pyridyldi-thio) propionate (SPDP), propan-2-ol, bicinchoninic acid (BCA) $HAuCl_4 \cdot 3H_2O$, and dimethylsulfoxide (DMSO) were obtained from Sisco Research Laboratory (SRL), Mumbai, India. Zeba spin desalting column was acquired from Thermo Fisher Scientific Inc. Milli-Q water was used to prepare all solutions. The whole blood samples of apparently healthy persons and diabetic patients were collected at Biodiagnostics Laboratory, Rohini, New Delhi.

2.2. Preparation of fructosyl valine (FV)

Due to the limited availability of FV, it was synthesized in our lab as reported earlier [25,26]. Briefly, 9.4 g of L-valine (0.16 mol) was added to 200 mL pyridine and 200 mL acetic acid and then the mixture was stirred for 30 min at room temperature. The solution was purged with nitrogen for 5 min after adding 40 g (0.22 mol) of glucose and then stirred for four days at 30 °C. The black color mixture was separated by filtration and the solvent was evaporated. After re-crystallization in methanol and then lyophilisation to a colorless precipitate, a slightly yellowish amorphous product was obtained.

2.3. Nanocomposites

TiO_2 NTs were synthesized as described by Yang et al. [27]. Hydroxyl activated NTs were prepared by combining polycrystalline TiO_2 with NaOH solution at 110 °C in a high pressure Teflon reactor for 20 h. 20 mL (10 mM) aqueous PTA solution and TiO_2 NTs (20 mg) were mixed and kept under constant stirring for 12 h. NTs were centrifuged and washed with distilled water to remove any uncoordinated PTA molecules. After adding 1 mL isopropanol to the suspension, it was purged with nitrogen for 15 min in a quartz cell. The solution was photoexcited for 4 h under four UV lamps (16 W, $\lambda ex = 253$ nm) to decrease the PTA from the TiO_2 NTs, then 5 mL of $HAuCl_4$ solution was added. The mixture was allowed to react for 2 h causing a transformation of the color of the mixture from dark blue to purple. The suspension was then centrifuged to obtain the GNPs- PTA-TiO_2 NTs.

2.4. Thiolation of FAO

Zeba desalt spin columns was used in the enzyme thiolation process contain a high-performance resin which offers exceptional purification, desalting and buffer exchange for protein samples. It does not required any chromatographic system and equilibration procedures or cumbersome preparation [9,28]. The thiolation of FAO was systematically carried out in steps. First, SPDP (1 mg) was dissolved in 160 μL of DMSO. This SPDP solution (12.5 μL) and 1 mg of FAO was dissolved in 500 μL of phosphate buffer saline containing 1 mM EDTA and was allowed to react for 30–60 min at 30 °C. To remove the storage solution, the desalt spin columns were centrifuged for 5 min at 2500 rpm. The acetate buffer was exchanged 2–3 times to equilibrate two desalting columns. The SPDP-modified FAO was centrifuged to get rid of reaction by products and the excess of non reacted SPDP. After that, 200 μL of DTT solution was added to 500 μL of SPDP-modified FAO solution and incubated for 30 min to synthesized thiolated FAO. The PBS-EDTA solution was used to equilibrate desalting columns. The excess of DTT was removed by desalted the thiolated FAO using the equilibrated columns.

Please cite this article in press as: U. Jain, et al., Glycated hemoglobin biosensing integration formed on Au nanoparticle-dotted tubular TiO_2 nanoarray, Analytica Chimica Acta (2016), http://dx.doi.org/10.1016/j.aca.2016.09.026

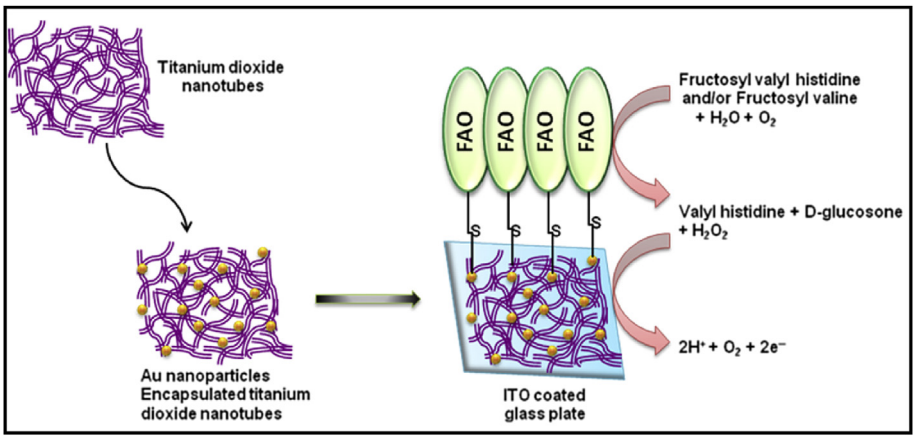

Scheme 1. Fabrication process of the FAO/GNPs-PTA-TiO_2 nanocomposite onto the ITO-coated glass plate and subsequent recognition of HbA_{1c}.

2.5. Preparation of a thiolated FAO biosensor

GNPs-PTA-TiO_2 nanocomposite was electrodeposited onto ITO coated glass plate electrode (2 cm × 1 cm) by cyclic voltammetry (CV). The ITO coated glass plate electrode was dipped in a 25 mL solution containing 22 mL electrolyte (2.5 mM $K_3Fe(CN)_6$/$K_4Fe(CN)_6$ [1:1]) and 3 mL nanoparticles (0.1 M KCl) and then −0.2 to +0.6 V was used for 20 cycles at a scan rate of 50 mV s^{-1}. The modified ITO electrode was washed with water to remove any unbound material. 20 μL of FAO solution was dispersed on the surface of the modified ITO electrode and kept at 4 °C for 24 h and then rinsed with distilled water. The working electrode (Scheme 1) was stored at 4 °C until use.

2.6. Response measurements of FAO/GNPs-PTA-TiO_2 nanocomposite modified ITO electrode

All electrochemical characterizations and measurements of the constructed biosensor were carried out by three electrode system. The system comprised of a Pt wire serving as the counter electrode and an Ag/AgCl electrode saturated with 3 M KCl was used as the standard electrode while the FAO/GNPs-PTA-TiO_2 nanocomposite modified ITO glass plate served as the working electrode. Measurements were conducted in an electrochemical cell containing 20 mL electrolyte [2.5 mM $K_3Fe(CN)_6$/$K_4Fe(CN)_6$ (1:1)], 5 mL potassium phosphate buffer (0.1 M, pH 7.0) and 0.1 mL of FV.

2.7. Optimization of FAO/GNPs-PTA-TiO_2 nanocomposite modified ITO electrode

The electrochemical response of an enzymatic biosensor depends on the type of electrolyte used. Two electrolytes, $K_3Fe(CN)_6$/$K_4Fe(CN)_6$ and KCl, were tested. Furthermore, in order to find out the optimum working conditions for the FAO/GNPs-PTA-TiO_2 nanocomposite modified ITO electrode, the pH of the reaction buffer (0.1 M) was varied from pH 5.0 to 9.0 at an interval of 0.5 using phosphate buffer (pH 5.0 to 7.0) and tris buffer (pH 7.5 to 9.0). Temperature of the reaction buffer was varied from 20 °C to 50 °C (in increments of 5 °C) for studying its effect on the biosensor response. Similarly, in order to determine the optimum response time, the current response was studied from 2 s to 20 s at an interval of 1s. The effect of substrate concentration was determined by varying the concentration of 0.5–2000 μM, which corresponds to physiological concentration of HbA_{1c} [29].

2.8. Detection of HbA_{1c} in samples (whole blood) using FAO/GNPs-PTA-TiO_2 nanocomposite modified ITO electrode

The whole blood samples of non-diabetic as well as diabetic patients (diagnosed by HPLC method) were collected from Biodiagnostics Laboratory, Rohini, New Delhi. All samples were mixed gently and then re-suspended the settled erythrocytes by inversion before use. Hemolysis of the sample was carried out by adding lysis buffer (Triton X 100, 100 mM CHES (pH 8.7), 1% SDS and 0.5 mM of oxidizing agent (dess martin periodinane) (250 μL) to 20 μL of whole blood sample, followed by incubation at 30 °C for 10 min). The lysis buffer was composed of Triton X 100, 100 mM CHES (pH 8.7), 1% SDS and 0.5 mM of dess martin periodinane. To ensure the release of amino acids, including glycated valines from the hemoglobin beta chains, blood samples were subjected to proteolytic digestion by adding 5 mM MES (4-Morpholino ethane sulfonic acid) (pH 7.0), 4 kU mL^{-1} purified *Bacillus* sp. proteases and 1 mM of oxidizing agent. The resulting mixture then served as a substrate for the enzyme (FAO). Another mixture composed of 0.1 M potassium phosphate buffer (pH 8.0), 90 U/mL peroxidase and 4-amino antipyrine (0.8 mM) was cleaved N-terminal amino acids either valine or histidine resulting in production of hydrogen peroxide (H_2O_2) [30].

Fructosylvaline, produced by proteolysis, undergoes N-terminal cleavage and is converted into either valine or histidine with concomitant formation of hydrogen peroxide (H_2O_2) by FAO in presence of 0.1 M potassium phosphate buffer (pH 8.0), 90 U/mL peroxidase and 4-amino antipyrine (0.8 mM).

$$\underset{(\beta-\text{chain N-terminal residue in } HbA_{1c})}{Fru-Val-His}-Leu-Thr-Pro-Glu-Glu-Lys-Ser\ldots \xrightarrow{\text{Protease}} \underset{(FV)}{\text{Fructosylvaline}} + \underset{(His,\ Leu,\ Thr)}{(\text{aminoacid})_{n-1}}$$

$$FV + O_2 + H_2O \xrightarrow{FAO} Valine + D-glucosone + H_2O_2$$

A standard curve was plotted using current values (μA) generated by the biosensor against % glycated hemoglobin in blood samples containing known amount of HbA_{1c} (as determined by the reference HPLC method). The generated calibration curve was used to determine HbA_{1c} concentration in unknown samples.

3. Results and discussion

The immobilizing of a scaffold made up of GNPs-modified TiO_2 NTs by using a linker (PTA) on the ITO electrode was performed. This leads to the fabrication of an electrochemical FAO biosensor. GNPs-modified TiO_2 NTs scaffold was then integrated with Thiolated FAO. PTA for synthesis of GNPs-TiO_2 composite was incorporated for the first time for obtaining uniformly dispersed GNPs, which causes a reduction of aggregated thiolated FAO resulting in immobilizing on the nanocomposite. Besides, PTA worked as an electron intermediary for direct electron transfer of FAO on the electrode. We further used various characterization techniques for individual components of the biosensor scaffold before applying thiolated FAO biosensor to detect HbA_{1c}.

3.1. Characterization of nanocomposites by TEM, XRD and UV-spectrophotometric spectra

Firstly, the morphology of synthesized TiO_2 NTs was characterized by TEM. In Fig. 1(A), TiO_2 display a tube like structure having diameter of about 50 nm and a length close to 100 nm TiO_2 provides a distinct environment which is biocompatible for enzymes entrapped in tiny dimensions comparatively better than other bulky TiO_2 nanomaterials such as TiO_2 nanoparticles and TiO_2 nanobundles [31].

Fig. 1(B) depicts the crystal framework of TiO_2 NTs and GNPs-PTA-TiO_2 nanocomposite, which were characterized by XRD. In the previous reports, a hydrothermal method was used to synthesize TiO_2 NTs showing a prominent feature with the diffraction peak at 2θ angle of 9° in trace (a) [32]. Furthermore, the peaks at 25.0°, 38.1°, and 48.5° correspond to the spacing of (101), (004), and (200) of the anatase (tetragonal) phase of the TiO_2 NTs [33]. Comparable to a previous report [34], the peaks at 38.3°, 44.6°, 64.8°, and 77.8° in trace c can be assigned to (110), (200), (220), and (311) reflection of GNPs, which clearly indicate that GNPs were successfully attached with TiO_2 NTs.

Fig. 1(C) depicts the UV–vis spectra of FAO, sulfhydryl-modified FAO, and sulfhydryl-modified FAO in the GNPs-PTA-TiO_2 nanotube scaffold. In this graph, the Soret band absorption for sulfhydryl-modified FAO (trace b) and FAO (trace a) were placed at similar wavelength (~403 nm) suggesting that the heme structure of FAO was not significantly altered after the thiolation process. Furthermore, after FAO was mixed with the GNPs-PTATiO_2 nanocomposite, no shift in the Soret band was observed (trace c). These nanocomposite materials furnish a remarkable biocompatibility and bioactivity resulting in retaining the native heme structure of FAO.

3.2. Evidences for various fabrication stages of FAO/GNPs-PTA-TiO_2 nanocomposite modified ITO electrode

The morphology of bare ITO electrode, GNPs-PTA-TiO_2/ITO electrode and FAO immobilized onto GNPs-PTA-TiO_2/ITO electrode were distinguished by SEM studies (Fig. 2). The smooth and plain morphology of the bare ITO electrode was shown in the SEM image

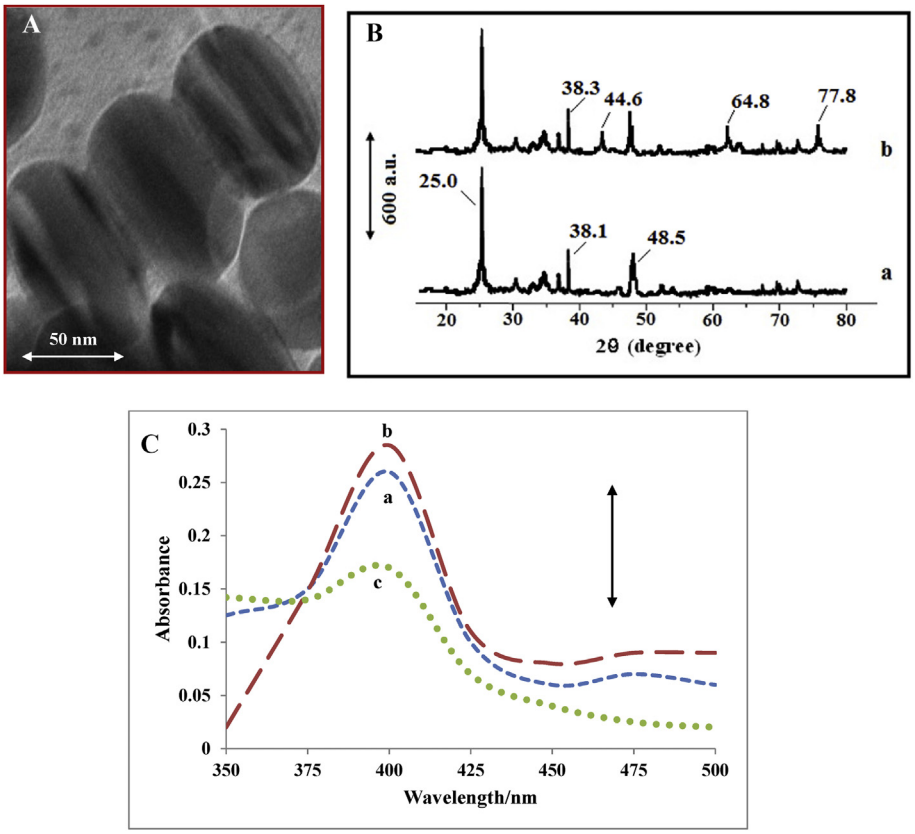

Fig. 1. (A) TEM images of TiO_2 NTs. (B) XRD pattern of (a) TiO_2 NTs and (b) GNPs-PTA-TiO_2 nanocomposite. (C) UV–vis absorption spectra of (a) FAO, (b) sulfhydryl modified FAO and (c) sulfhydryl modified FAO in GNPs-PTA-TiO_2 NTs composite.

Please cite this article in press as: U. Jain, et al., Glycated hemoglobin biosensing integration formed on Au nanoparticle-dotted tubular TiO_2 nanoarray, Analytica Chimica Acta (2016), http://dx.doi.org/10.1016/j.aca.2016.09.026

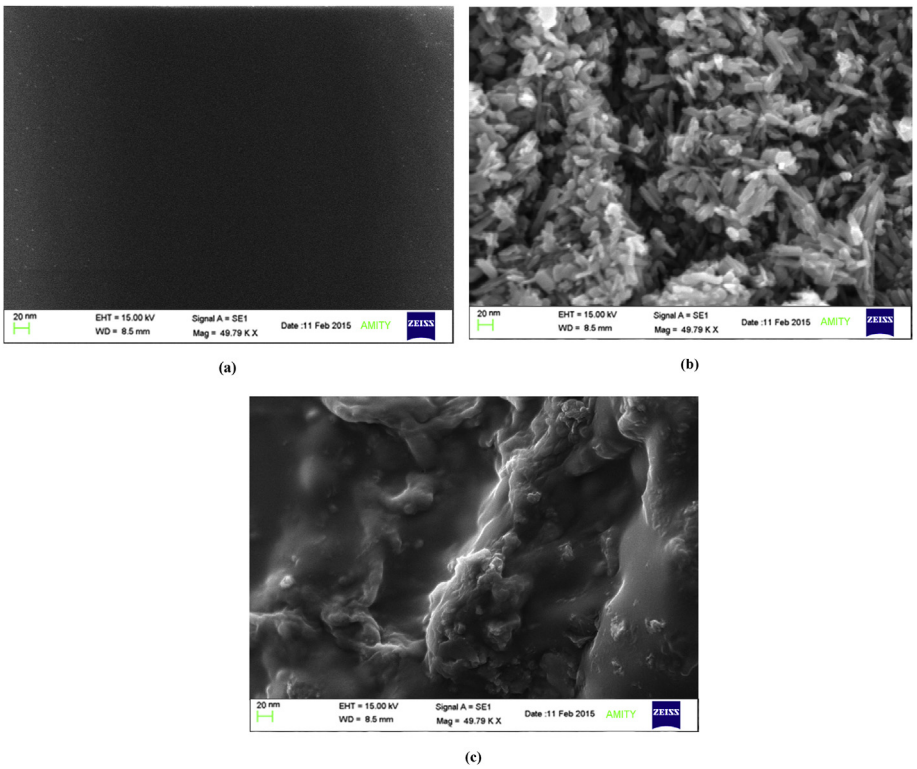

Fig. 2. SEM images of (a) bare ITO coated glass plate, (b) GNPs-PTA-TiO_2 nanocomposite onto the ITO coated glass plate (c) and FAO/GNPs-PTA-TiO_2 nanocomposite onto the ITO coated glass plate.

(image a). Fig. 2(b) displays usual SEM images of synthesized GNPs-PTA-TiO_2 hybrid nanocomposites revealing the structures which are highly densed and contain GNPs decorated TiO_2 nanorods. An effective attachment was obtained between TiO_2 nanorods and GNPs, providing a porous microstructure for the loading of proteins. As for the FAO/GNPs–TiO_2 composite (Fig. 2(c)), it can be seen that FAO was embedded into GNPs–TiO_2 nanocomposite with the increase of surface roughness. This indicates that FAO is intercalated into the layered structure of GNPs–TiO_2 nanocomposite.

The secondary structure of enzyme/protein was determined by FT-IR spectroscopy. At 1600–1700 cm^{-1}, the amide I band was determined which is due to the C═O extension and vibration of the peptide bond on FAO. The combination of N–H bending and C–N extension vibration of amide II band was obtained at 1500 and 1600 cm^{-1} [35,36], respectively. The structural alteration of an enzyme molecule is determined by the lack of intensity of these bands or even their disappearance [37]. As observed in Fig. 3A, the FT-IR spectrum results obtained before FAO thiolation (trace a) and taken after thiolation of FAO (trace b) were supported by the fact that no difference in the amide I and amide II bands was noticed. In addition, a very little change in the location and their intensity was observed once nanocomposite film was incorporated, which is shown in the amide I and amide II bands of FAO molecules (trace c). After the process of thiolation and entrapment of the nanocomposite material, the retention of the native secondary structure of FAO was confirmed. Since the heme group and secondary structure regulate the bioactivity of FAO, no major difference in bioactivity was visualized. This is confirmed by FT-IR showing non-detectable changes in the features of heme group and secondary structure.

The changes in interface surfaces on the electrode, occurred during the modification processes, were investigated by EIS. The

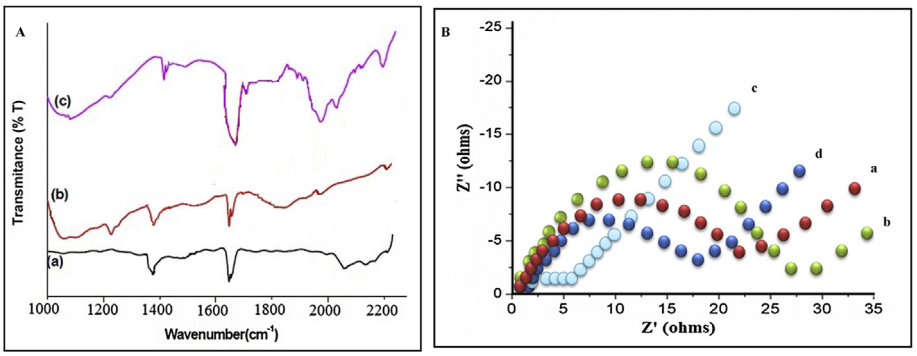

Fig. 3. A. FT-IR spectra of (a) FAO, (b) sulfhydryl modified FAO, and (c) sulfhydryl modified FAO in GNPs-PTA-TiO_2 NTs composite. B. Nyquist plots of 0.1 M KCl containing 10 mM $[Fe(CN)_6]^{3/4}$ from 0.1 MHz to 0.1 Hz at ac amplitude of 5 mV under open-circuit potential conditions, obtained at the bare ITO-coated glass plate (a), TiO_2 NTs onto the ITO-coated glass plate (b), GNPs-PTA-TiO_2 nanocomposite onto the ITO-coated glass plate (c) and FAO/GNPs-PTA-TiO_2 nanocomposite onto the ITO-coated glass plate incubated with FV (d).

Please cite this article in press as: U. Jain, et al., Glycated hemoglobin biosensing integration formed on Au nanoparticle-dotted tubular TiO_2 nanoarray, Analytica Chimica Acta (2016), http://dx.doi.org/10.1016/j.aca.2016.09.026

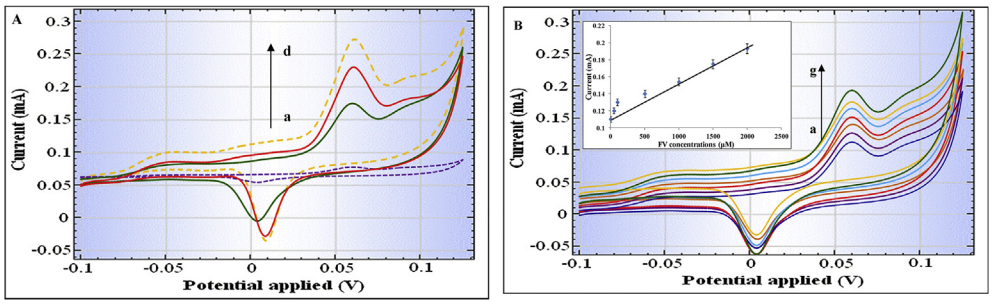

Fig. 4. A. Cyclic voltammograms of (a) bare ITO electrode, (b) TiO_2 nanocomposite onto the ITO electrode, (c) GNPs-PTA-TiO_2 nanocomposite onto the ITO electrode and (d) FAO/GNPs-PTA-TiO_2 nanocomposite onto the ITO electrode. B. (A) Cyclic voltammograms recorded at different concentrations of FV from 0.5 μM (a), 50 μM (b), 100 μM (c), 500 μM (d), 1000 μM (e), 1500 μM (f) and 2000 μM (g). Scan rate: 50 mV s^{-1} [Inset: Calibration curve for HbA_{1c} biosensor].

diverse electrodes were used to form the Nyquist plots by applying a probe having 0.1 M KCl with 10 mM $[Fe(CN)_6]^{3/4}$ (Fig. 3B). The bare ITO electrode reveals an electron transfer resistance (Rct) of approximately 23.0 Ω. The Rct value of 27.5 Ω was obtained for TiO_2 nanocomposite modified ITO electrode (curve b) which is decreased to 7.0 Ω after the modification of GNPs on GNPs-PTA-TiO_2 nanocomposite modified ITO electrode (curve c). This indicates that GNPs also had quick electron transfer kinetics between the electrode surface and electrolyte. In the FAO/GNPs-PTA-TiO_2 nanocomposite modified ITO electrode (curve d), the Rct value was increased to 19.0 Ω. The increase in RCT value is caused by the formation of implementation of enzyme molecules, resulting in obstacle of electron transfer by FAO.

3.3. Electrochemical response towards nanocomposite modified electrode

The potential range of −0.1 to +0.103 V was measured with separate modified electrodes, which is revealed by cyclic voltammograms in Fig. 4A. During these measurements, 0.1 M phosphate buffer at pH 7.5 was used with FV. In the beginning, no redox peak in the cyclic voltammogram (trace a) was observed while measuring at the ITO coated glass plate. The two components were incubated together for obtaining PTA-modified TiO_2 NTs. Furthermore, in order to get relatively appropriate quantity of PTA on the TiO_2 NTs, the copious rinsing procedure was performed. As a result, the signals obtained in the cyclic voltammogram (curve b) represented a detectable PTA. After immobilization of nanocomposite (GNPs-PTA-TiO_2), the redox peaks at 0.23 and −0.025 mA were acquired (curve c). The electron transfer between the electrolyte and the enzyme electrode was accelerated by GNPs and PTA forming a link between the two major components. GNPs and TiO_2 NTs provide a well suited environment for FAO. Trace d depicts the cyclic voltammogram of thiolated FAO after immobilization on the nanocomposite. An improvement was observed in the reduction to oxidation peak current ratio (from 0.23 (trace c) to 0.25 mA), which is shown in trace d. This improvement indicates a superior reversible capability through the direct electron transfer of FAO at the thiolated enzyme sensor.

3.4. Fabricated biosensor assessment

The fabricated biosensor was evaluated for the response of biosensor electrode system by change in FV concentration (0.5–2000 μM) which was found linear (Fig. 4B). The biosensor electrode system was able to detect (S/N = 3) upto 0.5 μM concentration showing a much lower detection limit while iridium nano-particle incorporated in the carbon-based working electrode [38], core–shell magnetic bionanoparticles modified gold electrode [39] and zinc oxide nanoparticles/polypyrrole hybrid film deposited on gold electrode [40].

The analytical recovery was studied after adding known concentration of exogenous FV to the serum sample. In order to calculate the analytical recovery (% recovery) of added FV, the HbA_{1c} concentration measurements were performed in the blood before and after addition of exogenous FV. The analytical recoveries obtained for two different concentrations 5 μM and 10 μM were 96.0% and 98.4% respectively. After evaluating measured analytical recoveries of added FV in the serum, it was observed that the prepared biosensor was very efficient. The within batch coefficient of variation (CV) for FV in the blood by our biosensor was 3.56% and for between batch, the CV was 4.25%. These traits reveal a reliable method of measurement and miscellaneous use of biosensor. For evaluating the accuracy of the current method, the HbA_{1c} values (in %) in 20 blood sample measurements (y) obtained by the prepared biosensor were compared with those measurements where standard HPLC method is used (x). After acquiring both values measured by biosensor and standard HPLC method, a correlation graph was plotted showing a very good correlation having R^2 = 0.9981 with regression equation, y = 0.9534x+0.3496 (Fig. 5A). The comparative analysis with the standard method and showing good correlation suggest that the present biosensor has good analytical performance for biological samples.

3.5. Optimization of experimental conditions

The FAO/GNPs-PTA-TiO_2/ITO electrode was evaluated for the optimum response where the conditions were set for temperature, pH, time and scan rate. 0.1 M FV solution was taken as standard for all the experimental conditions. The pH ranging from 5.0 to 9.0 was investigated. After evaluating the pH range, the maximum current response of the enzyme-catalyzed reaction was observed at pH 7.5. Thus, in our further experiments, pH of 7.5 was considered. The optimum response of biosensor was at 30 °C. The biosensor showed a maximum response (relatively faster) within 3 s. The change in scan rate for biosensor response was observed for 8 times (25–200 mV^{-1}). 0.1 M FV in 0.1 M potassium phosphate buffer solution (pH 7.5) was used. The scan rate of 50 mV^{-1} was taken as it exhibited a high potential. These experimental conditions collectively demonstrated the highest analytical performance and superior cyclic voltammogram profiles. The interfering substances at their physiological concentrations including bilirubin, ascorbic acid, cysteine, urea, uric acid, triglycerides and glucose were analyzed using current biosensor at 0.07 V versus Ag/AgCl in phosphate buffer at pH 7.5. Negligible interference was noticed which is calculated by decrease in percentage of biosensor response in the presence of these substances showing 2.36% for bilirubin, 3.41% for triglycerides, 4.63% for urea, 7.65% for ascorbic acid, 5.6%

Please cite this article in press as: U. Jain, et al., Glycated hemoglobin biosensing integration formed on Au nanoparticle-dotted tubular TiO_2 nanoarray, Analytica Chimica Acta (2016), http://dx.doi.org/10.1016/j.aca.2016.09.026

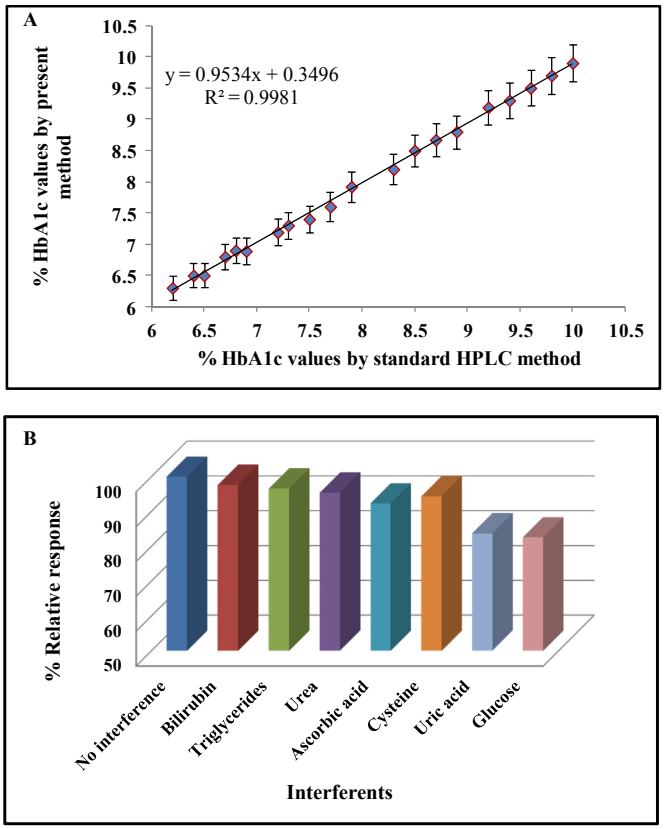

Fig. 5. A. Correlations between percentage HbA_{1c} values determined by standard immunoassay method (x-axis) and current FAO/GNPs-PTA-TiO_2 modified ITO electrode (y-axis). B. Effect of potential interferents on FAO/GNPs-PTA-TiO_2 nanocomposite onto the ITO electrode with 0.1 mM FV in 0.1 M sodium phosphate buffer (pH 7.5).

for cysteine, 16.27% for uric acid and 17.42% for glucose (Fig. 5B).

3.6. Glycated hemoglobin measurement in whole blood sample through FAO/GNPs-PTA-TiO_2/ITO electrode

The human whole blood samples were tested for HbA_{1c} levels measuring 4.3–5.8% (Supplementary Table 1). These measured values stipulate a standard range. The HbA_{1c} level was measured in the whole blood of diabetic patient by the prepared biosensor and was reported in the range of 6.2–9.9% (Supplementary Table 2). The HbA_{1c} levels were significantly higher in diabetic patients as compared to healthy persons (p value < 0.001). The excessive amount of glycation of b-chain of hemoglobin occurred in diabetic patients causing higher HbA_{1c} level in the blood resulting in an elevated level of blood glucose [41].

3.7. Long-term stability of electrode

The stability of FAO/GNPs-PTA-TiO_2/ITO electrode was examined in long-term, considering the importance of retention of the initial activity with respect to storage time. Firstly, in order to remove the possible interference caused by soluble proteins in the blood sample, the electrode was rinsed with reaction buffer for 3 times. During 120 days for 100 regular uses, the electrode retains 50% of its initial activity. In earlier reports, the initial activity was lesser as compared to prepared FAO biosensor. In these FAO biosensors iridium nano-particles were incorporated in the carbon-based working electrode [38], boronic acid modified gold substrate [42] and core–shell magnetic bionanoparticles modified gold electrode [39], (Supplementary Table 3). We suggest an efficient coupling method of nanocomposite material with the enzyme while covalently attached they maintain the immobilized FAO activity and prevent the electrode for leakage.

4. Conclusion

An electrochemical FAO biosensor was constructed which represents a novel strategy for developing a scaffold consisting of GNPs-PTA-TiO_2 NTs. PTA served as a reducing agent once after photo excited immobilized nanoparticles on TiO_2 nanotube surface were employed. Here, PTA also served as a speed up agent operating as an electron mediator throughout the process of enzyme catalysis. The scaffold modified working electrode showed fast response (3s), wide linear range (0.5–2000 μM), low detection limit (0.5 μM), good reproducibility (100 times), and long term stability (4 months). We were able to use this biosensor prototype successfully for HbA_{1c} detection in blood samples of diabetic patients.

Acknowledgement

One of the authors, Dr. Nidhi Chauhan got the financial assistance under the Young Scientist Scheme (Fast Track; File No. SB/YS/LS-106/2013). We would like to thank Science and Engineering Research Board (SERB), Department of Science and Technology (DST), New Delhi, for providing her the financial support for the project.

Appendix A. Supplementary data

Supplementary data related to this article can be found at http://dx.doi.org/10.1016/j.aca.2016.09.026.

References

[1] Y. Zou, D. Li, X. Sheng, L. Wang, D. Yang, Fabrication of TiO_2 nanorod array/semiconductor nanocrystal hybrid structure for photovoltaic applications, Sol. Energy 86 (2012) 1359–1365.
[2] L. Cano, A.E. Di Mauro, M. Striccoli, M.L. Curri, A. Tercjak, Optical and conductive properties of as-synthesized organic-capped TiO_2 nanorods highly dispersible in polystyrene-block-poly(methyl methacrylate) diblock copolymer, ACS Appl. Mater Interf. 23 (2014) 11805–11814.
[3] X. Wang, Z. Li, J. Shi, Y. Yu, One-dimensional titanium dioxide nanomaterials: nanowires, nanorods, and nanobelts, Chem. Rev. 114 (2014) 9346–9384.
[4] P. Photai, N. Grisdanurak, P. Khemthong, Structural properties of CuO/TiO_2 nanorod in relation to their catalytic activity for simultaneous hydrogen production under solar light, Int. J. Hydrogen Energy 38 (2013) 15992–16001.
[5] H. Fox, K.E. Newman, W.F. Schneider, S.A. Corcelli, Bulk and surface properties of rutile TiO_2 from self-consistent-charge density functional tight binding, J. Chem. Theory Comput. 6 (2010) 499–507.
[6] Z.D. Gao, Y. Qu, T. Li, N.K. Shrestha, Y.Y. Song, Development of amperometric glucose biosensor based on Prussian Blue functionalized TiO_2 nanotube arrays, Sci. Rep. 4 (2014) 6891–6897.
[7] Y. Zhang, P. Xiao, X. Zhou, D. Liu, B.B. Garcia, G. Cao, Carbon monoxide annealed TiO_2 nanotube array electrodes for efficient biosensor applications, J. Mater Chem. 19 (2009) 948–953.
[8] C. Feng, G. Xu, H. Liu, J. Lv, Z. Zheng, Y. Wu, Glucose biosensors based on Ag nanoparticles modified TiO_2 nanotube arrays, J. Solid State Electrochem. 18 (2014) 163–171.
[9] X. Liu, J. Zhang, S. Liu, Q. Zhang, X. Liu, D.K.Y. Wong, Gold Nanoparticle encapsulated-tubular TiO_2 nanocluster as a scaffold for development of thiolated enzyme biosensors, Anal. Chem. 85 (2013) 4350–4356.
[10] T.G.S. Babu, D. Varadarajan, G. Murugan, T. Ramachandran, B.G. Nair, Gold nanoparticle–polypyrrole composite modified TiO_2 nanotube array electrode for the amperometric sensing of ascorbic acid, J. Appl. Electrochem. 42 (2012) 427–434.
[11] N. Chauhan, J. Narang, C.S. Pundir, Immobilization of rat brain acetylcholinesterase on porous gold-nanoparticle–$CaCO_3$ hybrid material modified Au electrode for detection of organophosphorous insecticides, Int. J. Biol. Macromol. 49 (2011) 923–929.
[12] N. Chauhan, J. Narang, C.S. Pundir, Immobilization of lysine oxidase on a gold-platinum nanoparticles modified Au electrode for detection of lysine, Enzyme. Microb. Technol. 52 (2013) 265–271.

[13] N. Chauhan, J. Narang, C.S. Pundir, Immobilization of barley oxalate oxidase onto gold-nanoparticle-porous $CaCO_3$ microsphere hybrid for amperometric determination of oxalate in biological materials, Clin. Biochem. 45 (2012) 253–258.
[14] J.Y. Park, B.Y. Chang, H. Nam, S.M. Park, Selective electrochemical sensing of glycated hemoglobin (HbA1c) on thiophene-3-boronic acid self-assembled monolayer covered gold electrodes, Anal. Chem. 80 (2008) 8035–8044.
[15] B. Shanthi, C. Revathy, A. Jagdeeshwaran, M. DeviSubhashree, Effect of iron deficiency on glycation of haemoglobin in nondiabetics, J. Clin. Diagn. Res. 7 (2013) 15–17.
[16] N. Agarwal, S. Joshi, V.K. Deshpande, D.A. Biswas, Correlation between glycated haemoglobin and glucose testing for diabetes mellitus screening, Ind. J. Med. Res. 67 (2013) 149–154.
[17] W.G. John, M.R. Gray, D.L. Bates, J.L. Beacham, Enzyme immunoassay–a new technique for estimating hemoglobin A1c, Clin. Chem. 39 (1993) 663–666.
[18] J.O. Idemudia, E.O. Onovughakpo-Sakpa, E. Ayinbuomwan, B.E. Kasia, Measuring glycosylated haemoglobin (HBA1C): a Comparison of boronate affinity chromatographic method and spectrophotometric methods, Ann. Biomed. Sci. 10 (2011) 1–7.
[19] B. Moiz, M.R. Hashmi, S. Sadaf, Performance evaluation of ion exchange and affinity chromatography for HbA1c estimation in diabetic patients with HbD: a study of 129 samples, Clin. Biochem. 41 (2008) 1204–1210.
[20] J. Pribyl, P. Skládal, Development of a combined setup for simultaneous detection of total and glycated haemoglobin content in blood samples, Biosens. Bioelectron. 21 (2006) 1952–1959.
[21] A. Sahu, T. Gupta, P.D. Sarkar, Comparative study of nitro blue tetrazolium (NBT) reduction method for estimation of glycated haemoglobin with glycated HbA1c estimated on DCA2000+analyzer (immunoagglutination inhibition), J. Assoc. Physician Ind. 58 (2010) 20–22.
[22] R.R. Little, H. Vesper, C.L. Rohlfing, M. Ospina, S. Safar-Pour, W.L. Roberts, Validation by a mass spectrometric reference method of use of boronate affinity chromatography to measure glycohemoglobin in the presence of hemoglobin S and C traits, Clin. Chem. 51 (2005) 264–265.
[23] N. Chauhan, C.S. Pundir, Amperometric determination of acetylcholine – a neurotransmitter, by chitosan/gold-coated ferric oxide nanoparticles modified gold electrode, Biosens. Bioelectron. 61 (2014) 1–8.
[24] N. Chauhan, C.S. Pundir, An amperometric biosensor based on acetylcholinesterase immobilized onto iron oxide nanoparticles/multi-walled carbon nanotubes modified gold electrode for measurement of organophosphorous insecticides, Anal. Chim. Acta 701 (2011) 66–74.
[25] P. Keil, H.B. Mortensen, C. Christophersen, A simple model of the N-terminal residue of human haemoglobin A1c, Acta Chem. Scand. Ser. B Org. Chem. Biochem. 39 (1985) 191–193.
[26] R. Rajkumar, A. Warsinke, H. Mohwald, F.W. Scheller, M. Katterle, Development of fructosyl valine binding polymers by covalent imprinting, Biosens. Bioelectron. 22 (2007) 3318–3325.
[27] J.J. Yang, Z.S. Jin, X.D. Wang, W. Li, J.W. Zhang, S.L. Zhang, X.Y. Guo, Z.J. Zhang, Study on composition, structure and formation process of nanotube $Na_2Ti_2O_4(OH)_2$, Dalton Trans. 20 (2003) 3898–3901.
[28] X.Q. Liu, P.A. Duckworth, D.K.Y. Wong, Square wave voltammetry versus electrochemical impedance spectroscopy as a rapid detection technique at electrochemical immunosensor, Biosens. Bioelectron. 25 (2010) 1467–1473.
[29] K. Ogawa, D. Stollner, F. Scheller, A. Warsinke, F. Ishimura, W. Tsugawa, S. Ferri, K. Sode, Development of a flow-injection analysis (FIA) enzyme sensor for fructosyl amine monitoring, Anal. Bioanal. Chem. 373 (2002) 211–214.
[30] L. Liu, S. Hood, Y. Wang, R. Bezverkov, C. Dou, A. Datta, C. Yuan, Direct enzymatic assay for % HbA1c in human whole blood samples, Clin. Biochem. 41 (2008) 576–583.
[31] X. Liu, H. Feng, R. Zhao, Y. Wang, X. Liu, A novel approach to construct a horseradish peroxidase hydrophilic ionic liquids/Au nanoparticles dotted titanate nanotubes biosensor for amperometric sensing of hydrogen peroxide, Biosens. Bioelectron. 31 (2012) 101–104.
[32] Y. Wang, C.X. Feng, Z.S. Jin, J.W. Zhang, J.J. Yang, S.L. Zhang, A novel N-doped TiO_2 with high visible light photocatalytic activity, J. Mol. Catal. A Chem. 260 (2006) 1–3.
[33] X. Han, Y.H. Zhu, X.L. Yang, C.Z.J. Li, Electrocatalytic activity of Pt doped TiO_2 nanotubes catalysts for glucose determination, Alloys Compd. 500 (2010) 247–251.
[34] I. Paramasivam, J.M. Macak, P. Schmuki, Photocatalytic activity of TiO_2 nanotube layers loaded with Ag and Au nanoparticles, Electrochem. Commun. 10 (2008) 71–75.
[35] X. Sun, Y. Zhang, H. Shen, N. Jia, Direct electrochemistry and electrocatalysis of horseradish peroxidase based on halloysite nanotubes/chitosan nanocomposite film, Electrochim. Acta 56 (2010) 700–705.
[36] Z. Zhu, X. Li, Y. Wang, Y. Zeng, W. Sun, X. Huang, Direct electrochemistry and electrocatalysis of horseradish peroxidase with hyaluronic acid–ionic liquid–cadmium sulfide nanorod composite material, Anal. Chim. Acta 670 (2010) 51–56.
[37] Y.P. Song, M.C. Petty, J. Yarwood, W.J. Feast, J. Tsibouklis, S. Mukherjee, Fourier transform infrared studies of molecular ordering and interactions in Langmuir-Blodgett films containing nitrostilbene and stearic acid, Langmuir 8 (1992) 257–261.
[38] L. Fang, W. Li, Y. Zhou, C.-C. Liu, A single-use, disposable iridium-modified electrochemical biosensor for fructosyl valine for the glycosylated hemoglobin detection, Sens. Actuat. B 137 (2009) 235–238.
[39] S. Chawla, C.S. Pundir, An electrochemical biosensor for fructosyl valine for glycosylated hemoglobin detection based on core–shell magnetic bionanoparticles modified gold electrode, Biosens. Bioelectron. 26 (2011) 3438–3443.
[40] S. Chawla, C.S. Pundir, An amperometric hemoglobin A1c biosensor based on immobilization of fructosyl amino acid oxidase onto zinc oxide nanoparticles–polypyrrole film, Anal. Biochem. 430 (2012) 156–162.
[41] W. Azim, M. Omair, M.Q. Khan, N. Shaheen, S. Azim, Correlation between glycated haemoglobin and random plasma glucose levels for the screening of diabetes mellitus, Int. J. Path 8 (2010) 59–62.
[42] Kwang-Soo Ahn, Jung Hoon Lee, Jong-Myeon Park, Han Nim Choi, Won-Yong Lee, Luminol chemiluminescence biosensor for glycated hemoglobin (HbA1c) in human blood samples, Biosens. Bioelectron. 75 (2016) 82–87.

Please cite this article in press as: U. Jain, et al., Glycated hemoglobin biosensing integration formed on Au nanoparticle-dotted tubular TiO_2 nanoarray, Analytica Chimica Acta (2016), http://dx.doi.org/10.1016/j.aca.2016.09.026